

Determination of Terminal Velocity of Some Agricultural Grain Using Ansys Rocky DEM - CFD Coupling Simulation

Lemi Demissie Boset^{*}, Amana Wako, Biniam Zewdie

Department of Mechanical System and Vehicle Engineering, Adama Science and Technology University, Adama, Ethiopia

Email address:

lemidemissieboset@gmail.com (Lemi Demissie Boset)

^{*}Corresponding author

To cite this article:

Lemi Demissie Boset, Amana Wako, Biniam Zewdie. Determination of Terminal Velocity of Some Agricultural Grain Using Ansys Rocky DEM - CFD Coupling Simulation. *Science Development*. Vol. 4, No. 2, 2023, pp. 28-35. doi: 10.11648/j.scidev.20230402.12

Received: December 31, 2022; **Accepted:** June 9, 2023; **Published:** June 29, 2023

Abstract: Aerodynamic property of food grains are key elements in agricultural product harvesting, pneumatic conveying, separating, cleaning, transportation, and storage. Crop grain aerodynamic property influences the design and operational parameters of equipment. Among the property, terminal velocity is highly essential because it is crop variety specific and moisture dependant. Previously, the terminal velocity of agricultural grains could be evaluated experimentally using a vertical wind column equipment, but numerical analysis has recently emerged as the fastest and least expensive way for solving most of engineering problems. In this study, Rocky DEM was fully coupled with Ansys Fluent to model and simulate analysis of terminal velocity of Teff, wheat, Maize, Sorghum and Barley grains. after simulation results obtained comparison between experimental and simulation results based on previous researcher, from previous researchers terminal velocity of Teff, Wheat, Maize, Sorghum and Barley grains were 3.08-3.96m/s, 6.81-6.86m/s, 10.6-11.4m/s, 9.10-9.79m/s and 6.8-8.53m/s respectively at different moisture content, similarly for Ansys Rocky DEM-CFD coupling simulation result terminal velocity for Teff, Wheat, Maize, Sorghum and Barley grain were 3.6m/s, 9.1m/s, 10.8m/s, 9.6m/s and 6.6m/s respectively. Ansys RockyDEM-CFD coupling simulation results were almost the same with experimental result. To determine terminal velocity of any agricultural grain we can use experimental method or Ansys Rocky DEM-CFD coupling.

Keywords: Modeling, Simulation, Terminal Velocity, Physical Property, Grain, DEM-CFD Coupling

1. Introduction

1.1. Ansys Fluent and Rocky DEM-CFD Coupling

Due to its ability to preserve computational tractability while capturing the discrete nature of the particle phase, the linked DEM-CFD technique is a prospective substitute for modelling granular-fluid systems. In order to achieve this, the fluid flow problem is solved at the cell level as opposed to the fine-grained particle level. This method broadens the variety of equipment and processes that can be evaluated with numerical simulations by reducing the number of fluid calculations necessary. Tsuji et al. and Hoomans et al. were the first to report the coupling of DEM with a finite volume approach for the solution of fluid phase in a computational cell level, utilising the soft-sphere model and hard-sphere model for the interaction force.

Since then, several authors have published their research on granular flow using the Euler-Lagrange type of model. In

the DEM-CFD method, the fluid flow is determined using a discrete particle method, while the particle motion is determined using a typical continuum approach. This information is used to compute the fluid forces acting on individual particles. Below is a summary of some particular advantages of adopting the DEM-CFD linked approach over CFD alone, Interaction force, respectively, between particles.

- 1) Unlike continuum approaches, particle-particle interactions are taken into consideration because every particle's motion is modelled. Therefore, it is not necessary to present the difficult to construct equations for the state-motion of granular systems.
- 2) In the same vein, low particle size concentration is not a restriction, and particle size distribution can be easily prescribed without raising the computational cost of the CFD solver.
- 3) Dealing with non-spherical particles is possible.
- 4) By simulating the attractive force between two particles and between particles and walls, adhesive-cohesive

materials can be modelled.

- 5) The heat transmission between particles and their walls, as well as the convective heat transfer with the fluid, can also be taken into account [6].

1.2. Particle-Fluid Interaction Forces

The fluid interaction force, $F_{f \rightarrow p}$, is commonly split into two terms: the drag force, F_D , and a second term composed by the remaining (non-drag) forces, F_{N-D} , in the following way:

$$F_{f \rightarrow p} = F_D + F_{N-D}$$

Amongst the most common non-drag forces are the pressure gradient force, $F_{\Delta p}$, the added (virtual) mass force, F_{VM} and the lift force, F_L , so we could write also:

$$F_{f \rightarrow p} = F_D + F_{\Delta p} + F_L + F_{VM} + F_{others}$$

Only the drag and pressure gradient forces may need to be taken into account depending on the flow circumstances, such as when there is a significant specific mass difference between the fluid and the particles therefore ($\rho_p \gg \rho_f$).

$$F_{f-p} = F_D + F_{\Delta p}$$

1.3. Pressure Gradient Force

The pressure gradient force, $F_{\Delta p}$, is calculated according to the expression:

$$F_{\Delta p} = -V_p \Delta p$$

Where V_p is the volume of the particle and Δp is the local pressure gradient.

1.4. Drag Force

Unless specifically stated otherwise, the drag force, F_D , acting on the particles is calculated using the definition of the drag coefficient C_D

$$F_D = \frac{1}{2} C_D \rho_f A |u - v_p| (u - v_p)$$

Where $u - v_p$ is the relative velocity between particle and fluid and A is the projected particle area in the flow direction. Various drag correlations based on particle shape (spherical and non-spherical) and particle concentration (dilute or dense flows) are available within the Rocky package for the calculation of the drag coefficient. All correlations use the relative particle Reynolds number, R_{ep} , defined using the particle diameter and the relative particle-fluid velocity according to:

$$R_{ep} = \frac{\rho_f |v_p - u| d_p}{\mu_f}$$

1.5. Single Particle Drag Laws

A collection of correlations for the drag coefficient (drag laws) can be found in the extensive technical literature available on particle fluid interactions. Some of the most common and validated drag correlations for single particle (dilute flow) are implemented in the Rocky DEM-CFD coupling modules and apply to spherical and non-spherical particles.

1.6. Schiller & Naumann (1933)

The Schiller & Naumann drag correlation for spherical particles provides the drag coefficient C_D for $R_e < 800$ with a maximum deviation of 5% in relation to experimental data. The standard Pritchard, P. J. (2011). Fox and McDonald's Introduction to Fluid Mechanics. John version of the correlation is given by the research [17],

$$C_D = \frac{24}{R_{ep}} \left(1 + 0.15 R_{ep}^{0.687} \right)$$

A modification commonly used for inclusion of drag inertial range ($R_{ep} > 1000$) is given by:

$$C_D = \max \left[\frac{24}{R_{ep}} \left(1 + 0.15 R_{ep}^{0.687} \right), 0.44 \right]$$

The modified version of this drag law is implemented in Rocky DEM-CFD coupling, being the recommended drag law to be used for simulations with spherical particles.

1.7. DallaValle (1948)

The DallaValle drag law also provides the drag coefficient for spherical particles. Its validity range is up to $R_{ep} < 3000$ and its main difference to the modified Schiller & Naumann correlation is that it is a continuous function. The DallaValle correlation is defined by:

$$C_D = \left(0.63 + \frac{4.8}{\sqrt{R_{ep}}} \right)^2$$

1.8. Haider & Levenspiel (1989)

Haider & Levenspiel 12 compiled drag coefficient and terminal velocity experimental data for spherical and non-spherical particles. Then, they developed explicit expressions for both types of particles. For spherical particles, the correlation coefficients have fixed values whereas for non-spherical values they are dependent on the sphericity, which is defined below. The unified correlation for both types of particles is given by the research [5].

$$C_D = \frac{24}{R_{ep}} \left(1 + A R_{ep}^B \right) + \frac{C}{1 + \frac{D}{R_{ep}}}$$

For spherical particles, the values of the coefficients in this correlation are:

$$A = 0.1806$$

$$B = 0.6459$$

$$C = 0.4251$$

$$D = 6880.95$$

On the other hand, for non-spherical particles, they are given by the expressions:

$$A = \exp(2.3288 - 6.4581\phi + 2.4486\phi^2)$$

$$B = 0.0964 + 0.55565\phi$$

$$C = \exp(4.905 - 13.8944\phi + 18.4222\phi^2 - 10.2599\phi^3)$$

$$D = \exp(1.4681 + 12.2584\phi - 20.7322\phi^2 + 15.8855\phi^3)$$

Where ϕ is the particle's sphericity, defined as:

$$\phi = \frac{A_{sph}}{A_p}$$

Where A_{sph} is the surface area of a sphere having the same volume as the particle and A_p is the actual surface area of the particle.

As an illustration of the accuracy of this correlation, Figure below presents the comparison of equation with experimental data for spherical and distinct types of non-spherical particles, all with different values of sphericity.

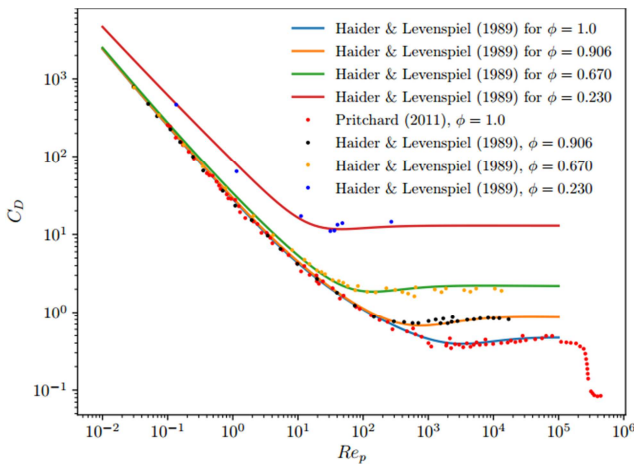


Figure 1. Comparison of the Haider & Levenspiel drag model for different sphericities to experimental data [9].

For non-spherical particles that can tolerate some accuracy loss and non-isometric non-spherical particles, the Haider & Levenspiel drag law is advised. Rocky determines the particle's sphericity based on the particle's size and shape.

1.9. One-Way Coupling Limitations

By definition, in a one-way coupling simulation, data is

transferred from one solution to another in only one direction. In this case the CFD solution provides information to the DEM solution, i.e., the fluid flow affects the particle trajectory but the particles do not affect the fluid flow. This is limited to situations where the particle loading is low and the coupling parameters are almost null. Please refer to the multiphase flow literature to evaluate these coupling parameters. Moreover, as currently implemented by Rocky, the setup of a one-way coupling simulation requires Fluent to export the steady-state solution of the CFD domain. This steady information of the fluid flow is employed by Rocky during the simulation there is no need of a companion Fluent process, since the steady-state of the CFD domain does not change with time. Therefore an intrinsic limitation of the one-way coupling with Fluent is that the transient state of the CFD domain is not simulated. Finally, the following conditions are verified by Fluent when exporting the steady-state solution to Rocky [4]:

- 1) Moving or adapting meshes are not supported.
- 2) Meshes with polyhedral cells around shadow boundaries are not supported.

1.10. Two-Way Coupling Limitations

By employing Fluent as described in section to simulate the transient state of the CFD domain as it is affected by the solidphase, the two-way coupling overcomes the limitations of the oneway coupling mentioned in section at the expense of being more computationally demanding. The following limitations apply to the current version of the two way DEM-CFD coupling module between Ansys Fluent and Rocky [4]:

- 1) Only 3D, unsteady and double precision Fluent cases are supported.
- 2) Fixed-time steps must be used (no time step adaptation).
- 3) Remeshing (creation or destruction of mesh elements) is not supported.
- 4) Meshes with polyhedral cells around shadow boundaries are not supported.
- 5) Fluent is not allowed to use GPUs.
- 6) Species Transfer and Finite-Rate Chemistry models are not supported.
- 7) Eulerian Wall Film model is not supported.
- 8) Dense Discrete Phase Model (DDPM) is not supported.
- 9) Boiling model is not supported.
- 10) Evaporation/Condensation model is not supported.
- 11) Multi-Fluid VOF model is not supported.
- 12) (Multiphase only) Multiphase Turbulence option must be set to Dispersed.
- 13) (Multiphase only) Both the Volume Fraction and Backflow Volume Fraction of the dispersed phase handling the particulate phase must be set to 0 at all boundaries.
- 14) (Multiphase only) Pressure-Velocity Coupling Scheme must be set to Phase Coupled SIMPLE.
- 15) Additional source terms in cell zones are not supported.
- 16) Fixed values in variables for cell zones are not supported.

17) All Rocky particle sets are combined to form a single equivalent Eulerian phase in Fluent [2].

2. Literature Review

Wheat kernel Bulk density ranged from 740 to 538.8 kg m³ at various moisture contents, showing a decline in bulk density as moisture content increased [13]. Physical properties often required for designing the equipments for planting, harvesting and postharvesting operations of seeds. Shiraz, Karoun, and Shiroudy are three well-known wheat cultivars. In 2007, the University of Tehran measured and analysed their physical characteristics for moisture content in 8, 12, and 18% w.b. At an average moisture content of 8% w.b., the average length, width, and thickness were 6.75, 3.26, and 2.77 mm, respectively. Studies on wheat seeds that had been rewetted revealed that the weight of a thousand kernels rose from 18.38 to 22.43g. At a moisture content of 8% w.b., the geometric and equivalent mean diameter, surface area, sphericity, and aspect ratio were 3.93, 3.94 mm, 48.68 mm, 0.58, and 0.48 respectively. The 2 porosity increased from 0.43 to 0.45%. Whereas the bulk density decreased from 0.72 to 0.66kg m and the -3 true density from 1.25 to 1.19 kg m, with an increasing in the moisture content range of 8 to 18% wb. The -3 static and dynamic angle of repose varied from 37.28 to 47.33 and 29.89 to 36.5. The mean of static friction coefficient of three wheat varieties increased the linearly against surfaces of three structural materials, namely, compressed plastic (0.43 - 0.53), galvanized iron (0.33 - 0.53) and plywood (0.35 - 0.41) as the moisture content increased from 8 to 18% w.b [7]. By increasing mass of the kernel from 0.02 to 0.05 g and moisture content from 7 to 20% (w.b.) Wheat kernel terminal velocity increased linearly from 7.04 to 7.74 m/s and 6.81 to 8.63 m/s, respectively [8].

We looked at the physical properties of tef (*Eragrostis tef* (Zucc.) Trotter) at moisture levels (w.b.) of 5.6%, 11.03%, 14.95%, 21.43%, 25.11%, and 29.6%. The length, width, equivalent sphere diameter, and mass of the thousand seeds increased from 1.01 to 1.27 mm, respectively, whereas the moisture content rose from 5.6% to 29.6% w.b. When the moisture content climbed from 5.6% to 21.43% and then again to 29.6%, the sphericity declined from 0.70 to 0.63 and then increased to 0.69. True and bulk densities dropped from 1361 to 1207 kg/m³ and 840 to 696 kg/m³, respectively [15, 16]. When the moisture content of Teff grains increased from 6.5% to 30.1% wet basis (w.b.), their terminal velocity increased linearly from 3.08 to 3.96 m/s [3].

Three kinds of sorghum, Taiz-7, Taiz-8, and Taiz-9, were examined for their physical features at three moisture content levels (10%, 15%, and 20% w.b.). Dimensions, sphericity, mass per thousand grains, particle and bulk density, porosity, and static coefficient of friction on three different surfaces

(plywood, galvanised iron, and stainless steel) were among the physical attributes measured. There have been established mathematical models that use moisture content as the independent variable and the change in physical attributes as the dependent variable. The average sorghum grain rose in length from 4.61 to 4.77 mm, width from 4.41 to 4.51 mm, thickness from 3.19 to 3.31 mm, and length from 2.74 to 2.86 mm, width from 4.14 to 4.26 mm, and thickness from 4.52 to 4.68 mm [1]. At a moisture content of 9.15% (wb), the engineering qualities of sorghum (*Sorghum bicolor* (L.) Moench) were ascertained. The average measurements for the three dimensions were 4.39 mm for length, 4.20 mm for breadth, and 2.64 mm for thickness. In terms of geometric mean diameter, sphericity, weight of a thousand grains, bulk density, and actual density, the average values were 3.64 mm, 0.834, 35.16 g, 812.4 kg/m³, and 1448.39 kg/m³, respectively [12].

In order to build the storage, handling, and processing facilities for agricultural products, physical property of grains must be taken into consideration. Using conventional methods, the physical and mechanical property of maize grains were assessed as a function of moisture content in the range of 10–30%. As the moisture content rose from 10 to 30%, the average size, sphericity, and density varied from 8.08 to 8.46 mm, 0.654 to 0.717, and 1219 to 886.47 kg/m³. The size of maize grains increased from 8.08 to 8.46 mm and sphericity from 0.654 to 0.717 with an increase in moisture content. From 634.85 kg/m³ to 650.81 kg/m³, the bulk density increased [14].

Physical properties of maize were evaluated as a function of moisture content. The obtained data provide help in the designing of post-harvest handling machinery. In the moisture range of 10 to 18% wet basis (w.b.), the length of the rewetted grain increased from 10.01 to 10.65 mm, width increased from 8.57 to 8.70 mm, thickness ranged from 4.63 to 4.97 mm, geometric mean diameter (GMD) increased from 7.34 to 7.67 mm, sphericity increased from 0.72 to 0.73, thousand kernel weight (TKW) increased from 258.1 to 287.9 g, bulk density decreased from 591.6 to 554.2 kg /m³ true density increased from 1194.9 to 1267.2 kg/m³. In the same moisture range the angle of repose varied from 23.36 to 28.55 for grain. Lightness (L) of grain ranges from 62.82 to 59.26, a value (red-green axis) ranges from 13.97 to 8.96, b value (yellow-blue axis) ranges from 31.05 to 26.19 and hue angle (z%) decreased from 14.59 to 14.06 with increase in moisture content of grain from 10 to 18% w.b [10].

The length increased from 8.10 to 8.62 mm, the width from 3.42 to 3.74 mm, the thickness from 2.61 mm to 2.84 mm, and the arithmetic and geometric diameter of seeds from 4.71 to 5.07 mm and from 4.16 to 4.50 mm, respectively. Several properties were studied in the moisture range from 13.15 to 45.82% dry basis [11].

Table 1. Engineering properties of some agricultural grains.

Cereal crop	Size			Bulk Density (kg/m ³)	True density (kg/m ³)	Terminal velocity (m/s)
	Length (mm)	Width/Diameter (mm)	Depth (mm)			
Wheat	5-9	2.91-3.72	2.60-3.14	538.8-740	1471-1465	6.81-8.63
Teff	1.01-1.27	0.59-0.68	0.71 - 0.87	696-840	1358.26 -1380	3.08- 3.96
Sorghum	4.61 - 4.77	4.41 -4.51	4.52- 4.68	824 -801	812.4 -1448.39	9.10-9.79
Maize	10.01-10.6	8.57 -8.70	4.63 -4.97	554.2-591.6	886.47- 1219	10.6-11.4
Barley	8.10 - 8.62	3.42 - 3.74	2.61 -2.84	721.1-758.9	1210.5 -1333.4	6.8 - 8.53

3. Method and Materials

3.1. Determination of Terminal Velocity Using Ansys Rocky DEM-CFD Coupling

Basic Physical properties of some agricultural grains are property and terminal velocity useful in grain cleaning and conveying processes. Determining physical properties of some agricultural grains, like the length, width, thickness, and terminal velocity of each grain variety will be determined for to model grain and simulation of Ansys Rocky DEM-CFD coupling.

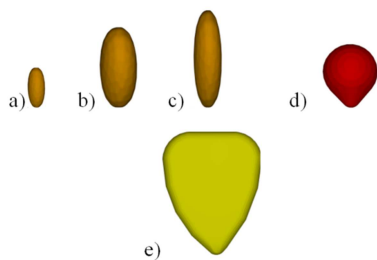


Figure 2. Rocky DEM modeled grains a) teff, b) wheat, c) barley, d) sorghum, and e) maize.

Data use for each grain for calibration of simulation analysis based on experimental result from previous works are as follows:

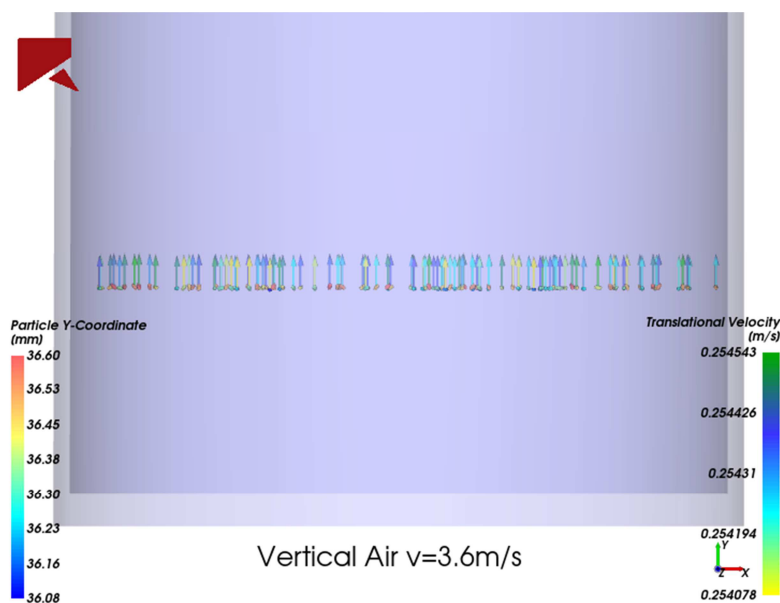
- 1) Physical property of teff kernel used for simulation

analysis are Length=1.2mm, Width=0.6mm, Depth=0.6mm, True density=1266.67kg/m³ and Bulk density =760kg/m³;

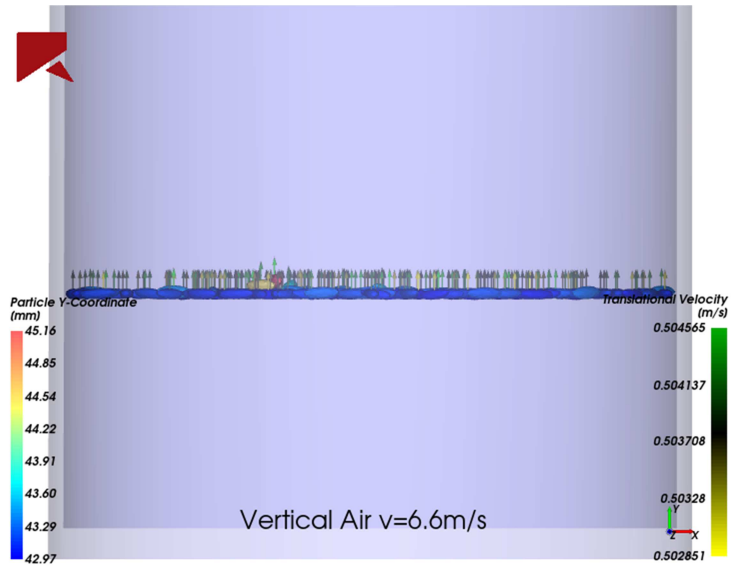
- 2) Physical property of barley kernel used for simulation analysis are Length=8.5mm, Width=3.6mm, Depth=2.8mm, True density=1210.51kg/m³ and Bulk density =730kg/m³;
- 3) Physical property of wheat kernel used for simulation analysis are Length=8.2mm, Width=3.4 mm, Depth=2.7mm, True density=1471 kg/m³ and Bulk density =1456kg/m³;
- 4) Physical property of sorghum kernel used for simulation analysis are Length=4.7mm, Width=4.5mm, Depth=4.5mm, True density=1350kg/m³ and Bulk density =812.4kg/m³;
- 5) Physical property of maize kernel used for simulation analysis are Length=10.5mm, Width=8.57mm, Depth=4.64mm, True density=980kg/m³ and Bulk density =560kg/m³.

3.2. Simulation Procedure

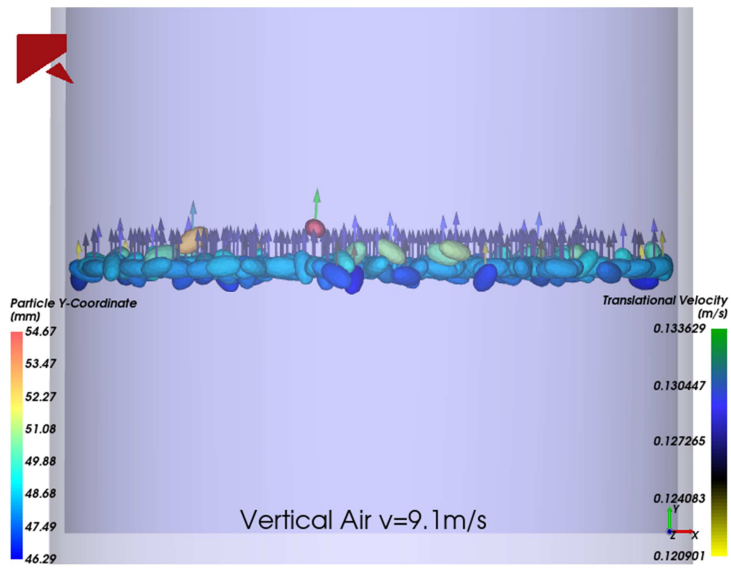
Step1 determine property of each grain, Step2 Model grain, Step3 Calibrate simulation, Step4 Simulate starting from minimum value of terminal velocity of grain referred from literature by adding small increments grain start suspended and terminal is obtained and Step5 after terminal velocity obtained the simulation result recorded as follows:



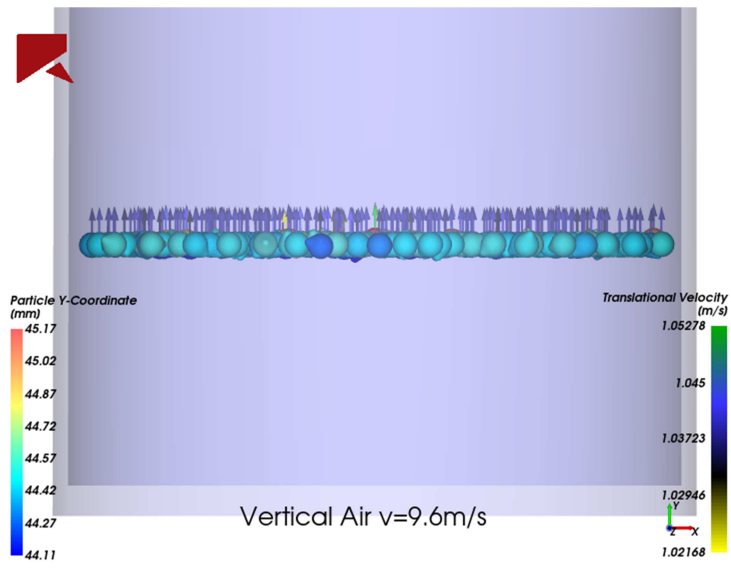
a)



b)



c)



d)

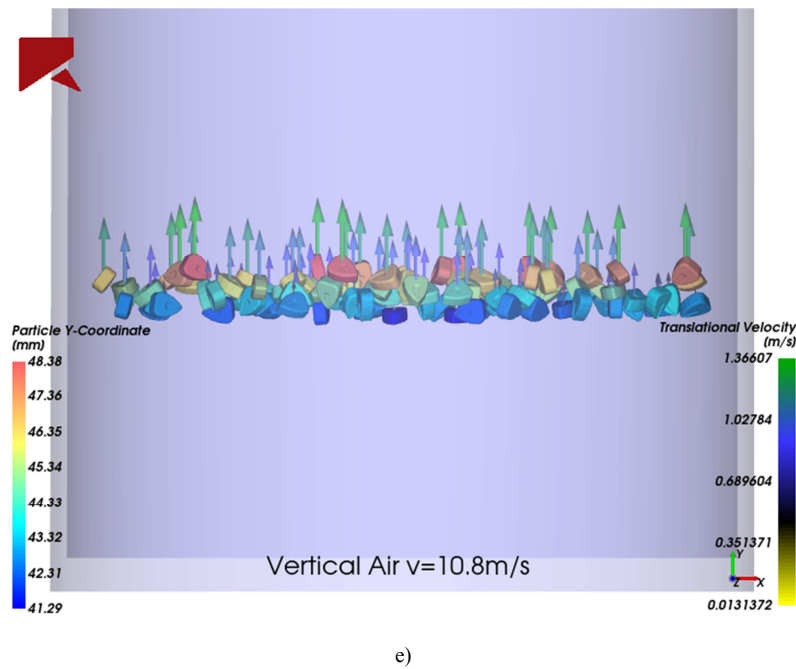


Figure 3. (a, b, c, d and e) are Terminal velocity of grains Ansys Rocky DEM-CFD coupling simulation result.

4. Result and Discussion

- 1) Figure 3.a) From simulation result of Ansys fluent rocky DEM-CFD coupling teff grain not fully suspended for air velocity $< 3.6\text{m/s}$ at 3.6m/s grain fully suspended in air stream and it is terminal velocity of teff grain.
- 2) Figure 3.b) From simulation result of Ansys fluent rocky DEM-CFD coupling barley grain not fully suspended for air velocity $< 6.6\text{m/s}$ at 6.6m/s grain fully suspended in air stream and it is terminal velocity of barley grain.
- 3) Figure 3.c) From simulation result of Ansys fluent rocky DEM-CFD coupling wheat grain not fully suspended for air velocity $< 9.1\text{m/s}$ at 9.1m/s grain fully suspended in air stream and it is terminal velocity of wheat grain.
- 4) Figure 3.d) From simulation result of Ansys fluent rocky DEM-CFD coupling sorghum grain not fully suspended for air velocity $< 9.6\text{m/s}$ at 9.6m/s grain fully suspended in air stream and it is terminal velocity of sorghum grain.
- 5) Figure 3.e) From simulation result of Ansys fluent rocky DEM-CFD coupling maize grain not fully suspended for air velocity $< 10.8\text{m/s}$ at 10.8m/s grain fully suspended in air stream and it is terminal velocity of maize grain.

5. Conclusion

The best thing about Ansys RockyDEM-CFD coupling is Rocky DEM has to be its speed and realistic modeling of any particle. This allows us to precisely simulate with the exact

number of particles size and shape. Because of crop grains are vary in size and complex in shape it is reasonable to use Rocky Dem for such kind of particle is method instead of using spherical particle based Dem software. Ansys RockyDEM-CFD coupling simulation result is almost the same with experimental result therefore it is another option to determine terminal velocity of any agricultural grain.

References

- [1] Abdul, Y., Qaid, G. & Al-mosanief, I., 2022. Effect of Moisture Content on Physical Characteristics of Sorghum Grains Yahya Abdul Galil Qaid Sallam and Ismael Al-mosanief., (5), pp. 5–20.
- [2] Technical Library - Rocky DEM – ESSS (2018). Ansys Fluent (CFD) and Rocky DEM coupling for modeling fluid particulate systems. <https://rocky.esss.co/blog/ansys-fluent-cfd-and-rocky-dem-coupling-for-modeling-fluid-particulate-systems/>
- [3] Awgichew, A., 2019. Aerodynamic Properties of Tef for Separation from Chaff. *Civil and Environmental Research*, 11 (3), pp. 39–43.
- [4] Copyright, C. O. M. & Reserved, A. R., 2015. Rocky dem user manual., pp. 1–211.
- [5] El-Emam, M. A. et al., 2021. *Theories and Applications of CFD-DEM Coupling Approach for Granular Flow: A Review*, Springer Netherlands. Available at: <https://doi.org/10.1007/s11831-021-09568-9>.
- [6] Guzman, L. & Chen, Y., 2020. Coupled CFD-DEM Simulation of Seed Flow in an Air Seeder Distributor Tube.
- [7] Karimi, M. et al., 2009. The effect of moisture content on physical properties of wheat. *Pakistan Journal of Nutrition*, 8 (1), pp. 90–95.

- [8] Khoshtaghaza, M. H. & Mehdizadeh, R., 2006. Aerodynamic Properties of Wheat Kernel and Straw Materials. *Agricultural Engineering International: the CIGR Ejournal*, VIII (January 2006), pp. 1–10.
- [9] Kuang, S., Zhou, M. & Yu, A., 2020. CFD-DEM modelling and simulation of pneumatic conveying: A review. *Powder Technology*, 365, pp. 186–207. Available at: <https://doi.org/10.1016/j.powtec.2019.02.011>.
- [10] Mi, G. et al., 2022. Measurement of Physical Properties of Sorghum Seeds and Calibration of Discrete Element Modeling Parameters.
- [11] Molenda, M. & Stasiak, M., 2001. Determination of the elastic constants of cereal grains in a uniaxial compression test. *International Agrophysics*, 16 (1), pp. 61–65.
- [12] Surpam, T., Pardeshi, I. & Rokade, H., 2019. Engineering properties of sorghum., 7 (5), pp. 108–110.
- [13] Tabatabaeefar, A., 2003. Moisture-dependent physical properties of wheat. *International Agrophysics*, 17 (4), pp. 207–211.
- [14] Yenge, G. et al., 2018. Physical Properties of Maize (*Zea mays* L.) Grain., (March 2019), pp. 3–7.
- [15] Zewdu, A. D., 2007. Aerodynamic properties of tef grain and straw material. *Biosystems Engineering*, 98 (3), pp. 304–309.
- [16] Zewdu, A. D. & Solomon, W. K., 2007. Moisture-Dependent Physical Properties of Tef Seed. *Biosystems Engineering*, 96 (1), pp. 57–63.
- [17] Zhou, H. et al., 2019. A novel, coupled CFD-DEM model for the flow characteristics of particles inside a pipe. *Water (Switzerland)*, 11 (11).